Volume 8, Issue 6, 2018, 3657 - 3660 ISSN 2069-5837

Biointerface Research in Applied Chemistry

www.BiointerfaceResearch.com

Original Research Article Open Access Journal

Received: 16.10.2018 / Revised: 28.11.2018 / Accepted: 04.12.2018 / Published on-line: 15.12.2018

Effect of Li, Na, K, Be, Mg and Ca on the electronic properties, geometrical parameters of carboxylic acids

Rania Badry [1], Alia S. A-E. Ghanem [1], Hend Ahmed [2], Ahmed Fahmy [2], Hanan Elhaes [1], Ahmed Refaat [2], Medhat Ibrahim [2]

[1]Physics Department, Faculty of Women for Arts, Science and Education, Ain Shams University, 11757 Cairo, Egypt
[2]Spectroscopy Department, National Research Centre, 33 El-Bohouth Str. 12622 Dokki, Giza, Egypt

*corresponding author e-mail address: ***medahmed6@yahoo.com***

ABSTRACT

A series of model molecules representing acetic acid (AA), substituted AA, benzoic acid (BA) and substituted BA have been optimized using quantum mechanical calculations. The studied structures were optimized at B3LYP/6-31G(d,p). The calculated total dipole moment (TDM) increased as a result of substitution in case of both AA and BA for Li, Na and K but decreased for Be, Mg and Ca. The band gap energy (HOMO/LUMO) is inversely proportional to TDM as it decreased by adding the studied elements to both AA and BA. Electrostatic potential results indicated that AA became more active when it was substituted with Na, and on the other hand BA became more active when it was substituted with K. Finally, the geometrical parameters such as bond length and angles are influenced by the substitutions.

Keywords: *Acetic acid, Benzoic acid, DFT, TDM, HOMO/LUMO band gap and ESP.*

1. INTRODUCTION

Acetic acid (AA) CH_3COOH is a member of carboxylic acids. Although it is a simple molecule, it plays an important role manifested by its continuous applications in different fields such as food, medicine, and chemistry [1-4]. Owing to its simple structure, it is always dedicated to functionalize other structures through carboxyl group [5]. Benzoic acid (BA) is the simplest aromatic carboxylic acid [6], well known as tracer from biomass burning [7], which has been found in smoke particles from residential wood combustion [8]. The carboxyl group is a well-known functional group with chemical reactivity. It is a group connecting unique hydrogen bonding considered as a bridge connecting organic and inorganic structures. It is one of the most reactive functional groups not only in chemistry but also in biology and the environment. Studying structures containing carboxyl group is an important step in organometallic interactions, biological interactions and environmental interactions [9-13]. The existence of carboxyl group in AA dedicates it as a model molecule for studying aliphatic structures containing carboxyl group [14-17]. The same is true for researchers who would like to model aromatic molecules containing carboxyl group so that they model BA as an ideal model molecule in their work [18-21]. Molecular modeling shows potential to study all classes of polymers as it is applied for synthetic polymers in this work and was previously applied for natural polymers [22-28]. In the present work, density functional theory (DFT) at B3LYP/6-31G(d,p) is utilized to calculate the effect of Li, Na, K, Be, Mg and Ca on the electronic properties and geometrical parameters of both AA acid and BA.

2. EXPERIMENTAL SECTION

Calculations Details. Model molecules are constructed for AA, substituted AA, BA and substituted BA with alkali and alkaline earth elements respectively. All model molecules are studied using GAUSSIAN09 program [29] at Spectroscopy Department, National Research Centre, Egypt and subjected to optimization with DFT at B3LYP/6-31g(d,p) level [30-32]. Total dipole moment (TDM), highest occupied molecular orbital and lowest unoccupied molecular orbital (HOMO/LUMO) band gap energy and electrostatic potentials (ESP) calculations are also performed using the same quantum mechanical calculations.

3. RESULTS SECTION

Two model molecules are designed with AA and BA as aliphatic and aromatic structures respectively containing carboxyl group. Each acid is supposed to be substituted with alkaline (Li, Na and K) and alkaline earth (Be, Mg and Ca). Substitution was done by replacing the H atom of the carboxyl group (COOH) of each acid. The model molecules presenting AA, substituted AA, BA and substituted BA are indicated in figures 1 and 2 respectively. As mentioned in previous researches, both TDM and HOMO/LUMO band gap energy ΔE can predict the ability of a specific molecule to interact with its neighbors [33,34]. Therefore, the study proceeds by calculating both TDM as Debye and HOMO/LUMO band gap energy ΔE as eV for all studied structures. Additionally, the reactivity of the studied structures is indicated with molecular ESP which is a measure of the points through which each structure is going to interact with the surrounding structures [35-37].

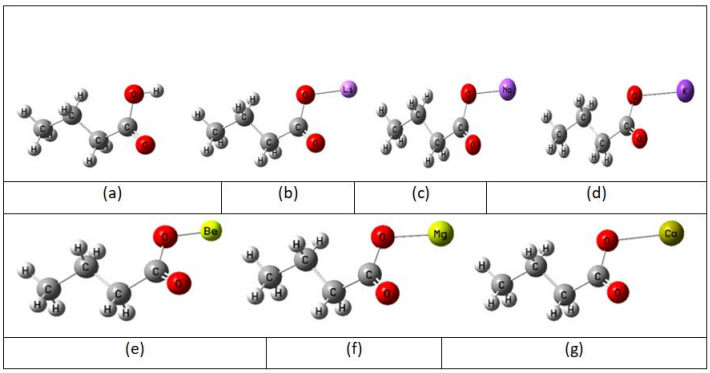

Figure 1. B3LYP/6-31g (d,p) optimized structure for a)AA, b)AA-Li, c)AA-Na, d)AA-K, e) AA-Be, f) AA-Mg and g) AA-Ca.

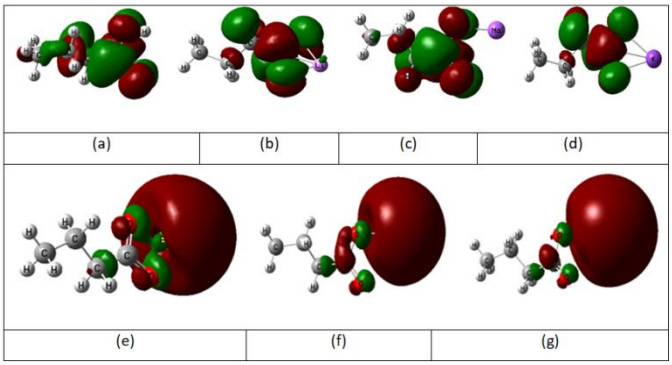

Figure 2. B3LYP/6-31g (d,p) HOMO/LUMO band gap energy for a) AA, b) AA-Li, c) AA-Na, d) AA-K, e) AA-Be, f) AA-Mg and g) AA-Ca.

The B3LYP/6-31g(d,p) calculated parameters are listed in table 1. In the case of AA, the TDM increased with increasing the atomic number of the studied elements; the TDM increased from 1.7591 Debye to a maximum value of 7.5198 Debye which is for substituted AA with K, while the HOMO/LUMO band gap energy decreased from 7.6157 eV to 3.4561 eV which is for AA substituted with Na. The TDM also increased as a result of substitution of AA with alkaline earth metals, reaching a maximum of 3.5570 Debye which is for AA substituted with Be, and the HOMO/LUMO band gap energy also decreased with increasing the atomic number of the metals which decreased to a minimum of 1.7456 eV for AA substituted with Ca.

Table 1. B3LYP/6-31G (d,p) calculated total dipole moment (TDM) as Debye; HOMO/LUMO band gap energy (ΔE) as eV for the studied structures: a: AA, b: AA-Li, c: AA-Na, d: AA-K, e: AA-Be, f: AA-Mg and g: AA-Ca.

Structure	TDM	ΔE
AA	1.7591	7.6157
AA-Li	3.2556	5.9253
AA-Na	6.9288	3.4561
AA-K	7.5198	4.1441
AA-Be	3.5570	3.2205
AA-Mg	2.2977	2.3301
AA-Ca	3.5146	1.7456

The molecular ESP was calculated at the same level of theory. ESP is depicted as contour and as total surface area for all model molecules under study. Figures 3 and 4 present ESP as contour and as total surface area respectively for all models. ESP, similar to TDM and HOMO/LUMO band gap energy, also depicts the reactivity of different structures and helps us to decide which site is the most suitable for interactions.

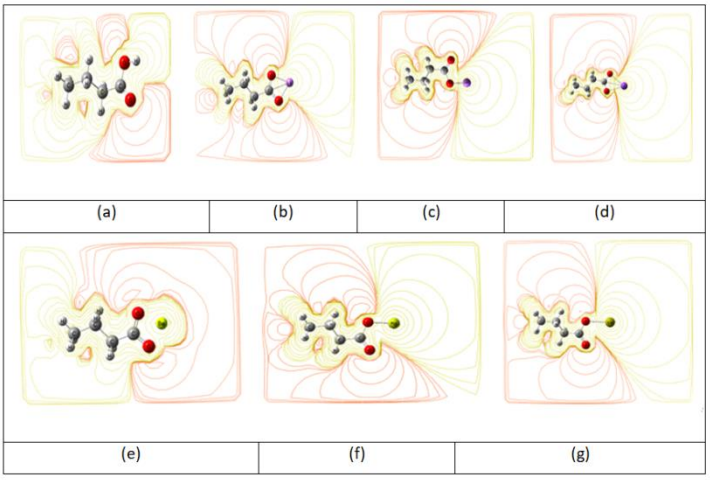

Figure 3. B3LYP/6-31g (d,p) ESP as contour for a) AA, b) AA-Li, c) AA-Na, d) AA-K, e) AA-Be, f) AA-Mg and g) AA-Ca.

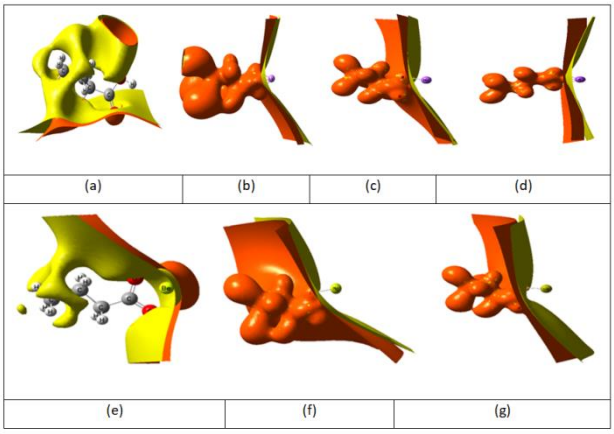

Figure 4. B3LYP/6-31g (d,p) ESP as total surface for a) AA, b) AA-Li, c) AA-Na, d) AA-K, e) AA-Be, f) AA-Mg and g) AA-Ca.

Besides the calculations of AA, the same calculations are also performed for BA and substituted BA with the same substitutions mentioned before. Figure 5 and 6 present the optimized structures and HOMO/LUMO band gap energy for BA, BA-Li, BA-Na, BA-K, BA-Be, BA-Mg and BA-Ca respectively.

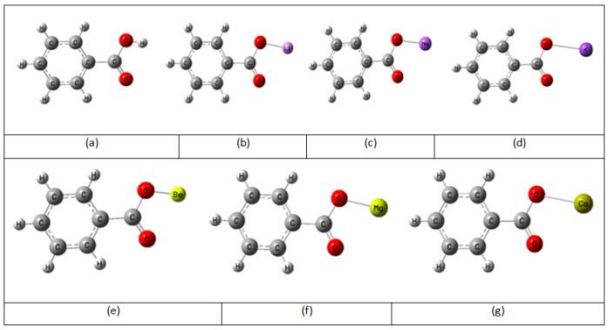

Figure 5. B3LYP/6-31g (d,p) optimized structure for a) BA, b) BA-Li, c) BA-Na, d) BA-K, e) BA-Be, f) BA-Mg and g) BA-Ca.

Table 2 illustrates the changes occurred in both TDM and HOMO/LUMO band gap energy as a result of substitutions of BA with the same elements. As a consequence of interactions, TDM increased with increasing the atomic number of alkali metals group from 1.9152 Debye to a maximum of 7.9326 Debye which is for BA substituted with K and decreased with increasing that of alkaline earth metals group, reaching a minimum of 0.4414 Debye for BA substituted with Ca, which means that Ca is almost inactive. On the other hand, the band gap energy decreased with increasing the atomic number for both groups but the decrease in

the case of Be, Mg and Ca is higher than that for Li, Na and K as it decreased from 5.7797 eV to 4.3318 eV for alkali group and to 1.7639 eV for alkaline group. The ESP for BA and substituted BA was also calculated at the same level of theory. Figures 7 and 8 present the ESP as contour and as total surface area for BA, BA-Li, BA-Na, BA-K, BA-Be, BA-Mg and BA-Ca.

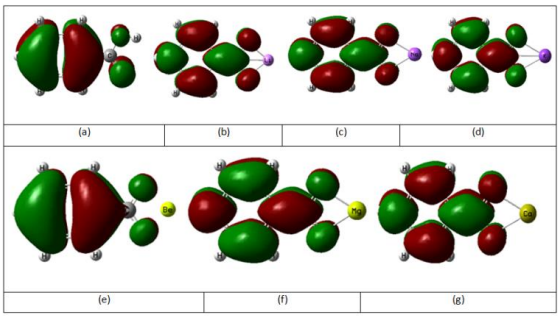

Figure 6. B3LYP/6-31g (d,p) HOMO/LUMO band gap energy for a) BA, b) BA-Li, c) BA-Na, d) BA-K, e) BA-Be, f) BA-Mg and g) BA-Ca.

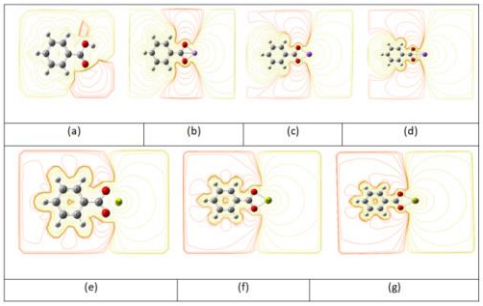

Figure 7. B3LYP/6-31g (d,p) ESP as contour for a) BA, b) BA-Li, c) BA-Na, d) BA-K, e) BA-Be, f) BA-Mg and g) BA-Ca.

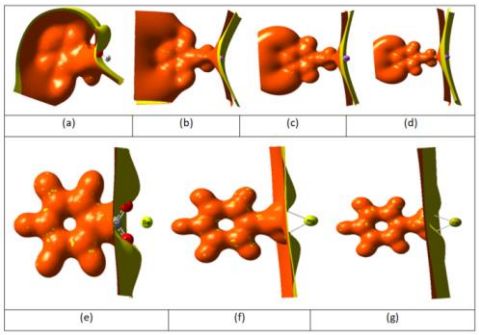

Figure 8. B3LYP/6-31g (d,p) ESP as total surface for a) BA, b)BA-Li, c) BA-Na, d) BA-K, e) BA-Be, f)BA-Mg and g) BA-Ca.

Other good results of these calculations are the bond length and bond angle, where tables 3 and 4 present the change in bond length and bond angle for both AA and BA with their substitution metals. The bond lengths and bond angles increased with increasing the atomic number. For AA, the bond length increased with increasing the atomic number of metals of the same group, such that it increased from 0.9722 Å for AA to 1.8546, 2.0600 and 2.5190 Å for AA substituted with Li, Na and K respectively, while the bond angle changed from 105.878° for AA to 82.412°, 109.471° and 90.847° for AA substituted with Li, Na and K respectively. Whereas for AA substituted with Be, Mg and Ca, the bond length is also changed upon substitution and increased to 1.6697, 2.0200 and 2.4000 Å for Be, Mg and Ca. The bond angle also changed to 82.509°, 109.471° and 109.471°. Similarly, the bond length for BA changed and also increased but the bond angle decreased by adding the studied metals to BA. The bond length increased from 0.9714 Å for BA to 1.8539, 2.1819, 2.5212, 1.6597, 2.0522 and 2.3511 Å for BA-Li, BA-Na, BA-K, BA-Be, BA-Mg and BA-Ca respectively. The bond angle for the same structures decreased from 105.617° for BA to 82.583°, 87.122°, 91.030°, 82.748°, 87.690° and 90.936° for BA-Li, BA-Na, BA-K, BA-Be, BA-Mg and BA-Ca respectively.

Table 2. B3LYP/6-31G (d,p) calculated total dipole moment (TDM) as Debye; HOMO/LUMO band gap energy (ΔE) as eV for the studied structures: a: BA, b: BA-Li, c: BA-Na, d: BA-K, e: BA-Be, f: BA-Mg and g: BA-Ca.

Structure	TDM	ΔE
BA	1.9152	**5.7797**
BA-Li	3.0630	**5.6989**
BA-Na	5.6898	**4.7090**
BA-K	7.9326	**4.3318**
BA-Be	4.7637	**2.0809**
BA-Mg	1.3265	**2.4354**
BA-Ca	0.4414	**1.7639**

Table 3. B3LYP/6-31G (d,p) calculated bond length as Angstroms and bond angle as Degree for the studied structures: a: AA, b: AA-Li, c: AA-Na, d: AA-K, e: AA-Be, f: AA-Mg and g: AA-Ca where X= H, Li, Na, K, Be, Mg and Ca.

Structure	Bond length (O3-X14)	Bond angle (C1 O3 X14)
AA	0.9722	105.878
AA-Li	1.8546	82.412
AA-Na	2.0600	109.471
AA-K	2.5190	90.847
AA-Be	1.6697	82.509
AA-Mg	2.0200	109.471
AA-Ca	2.4000	109.471

4. CONCLUSIONS

DFT level of theory proves to be effective in studying and following up the structural and electronic properties of both aliphatic and aromatic carboxylic, and is in a good agreement with previous work applied for different other materials [37-41].

A series of model molecules of AA, substituted AA, BA and substituted BA are optimized at B3LYP/6-31G (d,p). As a result of substitution and since the increase in TDM in case of alkali metals is higher than that of alkaline earth metals, it is clear that Li, Na and K are more reactive than Be, Mg and Ca, and especially Na is the most active metal for substitution with AA in comparison with the other studied alkali metals as TDM equals 6.9288 Debye and HOMO-LUMO band gap energy equals 3.4561 eV, while K is the most active metal for substitution with BA as TDM equals 7.9326 Debye and HOMO-LUMO band gap energy equals 4.3318 eV. Additionally, when AA and BA are substituted with alkaline earth metals, we concluded that Ca and Be are the much more active metals when Ca interacts with AA and Be interacts with Be, as TDM for both cases equals 3.5146 and 4.7637 Debye respectively, and HOMO-LUMO band gap energy equals 1.7456 and 2.0809 eV respectively. Another good agreement with TDM and band gap energy values are the values of bond length that were higher for Li, Na and K than for Be, Mg and Ca for both AA and BA substitution.

5. REFERENCES

[1] Rinaudo M., Pavlov G., Desbrières J., Influence of acetic acid concentration on the solubilization of chitosan, *Polymer*, 40, 7029-7032, **1990**.

[2] Singh V., Sehgal A., Parashari A., Sodhani P., Satyanarayana L., Early detection of cervical cancer through acetic acid application—an aided visual inspection, *Singapore Med J.*, 42, 8, 351-354, **2001**.

[3] Vlieger D.J.M.D., Lefferts L., Seshan K., Ru substituted carbon nanotubes–a promising catalyst for reforming bio-based acetic acid in the aqueous phase, *Green Chem*., 16, 864-874, **2014.**

[4] Sankaranarayanan R., Wesley R., Somanathan T., Dhakad N., Shyamalakumary B., Amma N.S., Parkin D.M., Nair M.K., Visual inspection of the uterine cervix after the application of acetic acid in the detection of cervical carcinoma and its precursors, *Cancer*, 83, 2150-2156, **1998.**

[5] Lee S.D., Hsiue G.H., Chang P.C.T., Kao C.Y., Plasma-induced grafted polymerization of acrylic acid and subsequent grafting of collagen onto polymer film as biomaterials, *Biomaterials*, 17, 1599-1608, **1996.**

[6] Simoneit B.R.T., Biomass burning – a review of organic tracers for smoke from incomplete combustion, *Appl. Geochem*., 17, 129-162, **2002.**

[7] Fine P.M., Cass G.R., Simoneit B.R.T., Chemical characterization of fine particle emissions from fireplace combustion of woods grown in the Northeastern United States, *Environ. Sci. Technol*., 35, 2665-2675, **2001.**

[8] Neumüller O. –A., Römpp (Eds) H., Römpps Chemie-Lexikon: Bd. 6: T-Z, Franckh, *Stuttgart*, **1988.**

[9] Ibrahim M., Koglin E., Vibrational Spectroscopic Study of Acetate Group, *Acta Chim. Slov*., 51, 453-459, **2004.**

[10] Ibrahim M., Nada A., Kamal D-E., DFT and FTIR Spectroscopic Study of Carboxyl Group, *Indian Journal of Pure and Applied Physics*, 43, 911-917, **2005.**

[11] Ibrahim M., El-Haes H., Computational Spectroscopic Study of Copper, Cadmium, Lead and Zinc Interactions in the Environment, *Int. J. Environ. Pollut*., 23, 417-424, **2005.**

[12] Ibrahim M., Molecular Modelling and FTIR Study for K, Na, Ca and Mg Coordination with Organic Acid, *J. Comput. Theor. Nanosci*., 6, 682–685, **2009**.

[13] Ibrahim M., Mahmoud A-A., Computational Notes on the Reactivity of some Functional Groups, *J. Comput. Theor. Nanosci*., 6, 1523–1526, **2009**.

[14] Verma A.M., Kishore N., Decomposition of acetic acid over Ru and Ru/MgO catalyst clusters under DFT framework, *Chem. Phys. Lett*., 711, 156-165, **2018.**

[15] Hossain M.A., Jewaratnam J., Ramalingam A., Sahu J.N., Ganesan P., A DFT method analysis for formation of hydrogen rich gas from acetic acid by steam reforming process, *Fuel*, 212,, 49-60, **2018.**

[16] Sienkiewicz-Gromiuk J., DFT approach to (benzylthio)acetic acid: Conformational search, molecular (monomer and dimer) structure, vibrational spectroscopy and some electronic properties, *Spectrochim. Acta A*, 189, 116-128, **2018**.

[17] Tavares S.R., Wypych F., Leitão A.A., DFT-based calculations of the adsorptions of acetic acid, triacetin, methanol and the alkoxide formation on the surfaces of zinc acetate, *Molecular Catalysis*, 440, 43-49, **2017.**

[18] Santhy K.R., Sweetlin M.D., Muthu S., Kuruvilla T.K., Abraham C.S., Structure, spectroscopic study and DFT calculations of 2,6 bis (tri fluro methyl) benzoic acid, *J. Mol. Struct*., 1177, 401-417, **2019.**

[19] Suo Y., Liu H., Huang S., Zhang Y., Ding K., The functionalization effect of benzoic acid and anisole on the photocatalytic activity of monolayer MoS_2, *Appl. Surf. Sci*., 437, 314-320, **2018.**

[20] Pramanik S., Dey T., Mukherjee A.K., Five benzoic acid derivatives: Crystallographic study using X-ray powder diffraction, electronic structure and molecular electrostatic potential calculation, *J. Mol. Struct*., 1175, 85-194, **2019.**

[21] Zhang L., Wang Q., Spectroscopic and first principles investigation on 4-[(4-pyridinylmethylene)amino]-benzoic acid bearing pyridyl and carboxyl anchoring groups, *J. Mol. Struct*., 1155, 389-393, **2018.**

[22] Ammar N.S., Elhaes H., Ibrahim H.S., El-Hotaby W., Ibrahim M.A., A Novel Structure for Removal of Pollutants from Wastewater, *Spectrochim. Acta A*. 121C, 216-223, **2014.**

[23] Ibrahim M., Saleh N.A., Elshemey W.M., Elsayed A.A., Hexapeptide Functionality of Cellulose as NS3 Protease Inhibitors, *Med. Chem.*, 8, 826-830, **2012.**

[24] Ibrahim M., Osman O., Spectroscopic Analyses of Cellulose: Fourier Transform Infrared and Molecular Modelling Study, *J. Comput. Theor. Nanosci*., 6, 1054–1058, **2009.**

[25] Abdelsalam H., Elhaes H., Ibrahim M.A., First principles study of edge carboxylated graphene quantum dots, *Physica B*, 537, 77-86, **2018.**

[26] Abdelsalam H., Elhaes H., Ibrahim M.A., Tuning electronic properties in graphene quantum dots by chemical functionalization: Density functional theory calculations, *Chem. Phys. Lett*., 695, 138-148, **2018.**

[27] Elhaes H., Osman O., Ibrahim M., Interaction of Nano Structure Material with Heme Molecule: Modelling Approach, *J. Comput. Theor. Nanosci.*, 9, 901–905, **2012.**

[28] Gaussian 09, Revision C.01, Frisch M., Trucks G., Schlegel H., Scuseria G., Robb M., Cheeseman J., Scalmani G., Barone V., Mennucci B., Petersson G., Nakatsuji H., Caricato M., Li X., Hratchian H., Izmaylov A., Bloino J,, Zheng G., Sonnenberg J., Hada M., Ehara M., Toyota K., Fukuda R., Hasegawa J., Ishida M., Nakajim T., Honda Y., Kitao O., Nakai H., Vreven T., Montgomery J., Peralta J.Jr., Ogliaro F., Bearpark M., Heyd J., Brothers E., Kudin K., Staroverov V., Keith T., Kobayashi R., Normand J., Raghavachari K., Rendell A., Burant J., Iyengar S., Tomasi J., Cossi M., Rega N., Millam J., Klene M., Knox J., Cross J., Bakken V., Adamo C., Jaramillo J., Gomperts R., Stratmann R., Yazyev O., Austin A., Cammi R., Pomelli C., Ochterski J., Martin R., Morokuma K., Zakrzewski V., Voth G., Salvador P., Dannenberg J., Dapprich S., Daniels A., Farkas O., Foresman J,, Ortiz J., Cioslowski J,, Fox D., Gaussian, Inc., *Wallingford CT*, **2010.**

[29] Becke A.D., Density-functional thermochemistry. III. The role of exact exchange, *Chem. Phys*., 98, 5648-5652, **1993.**

[30] Lee C., Yang W., Parr R.G., Development of the Colle-Salvetti correlation-energy formula into a functional of the electron density, *Phys. Rev. B.*, 37, 785-789, **1988.**

[31] Miehlich B., Savin A., Stoll H., Preuss H., Results obtained with the correlation energy density functionals of Becke and Lee, Yang and Parr, *Chem. Phys. Lett*., 157, 200-206, **1989.**

[32] Ibrahim M., El-Haes H., Computational Spectroscopic Study of Copper, Cadmium, Lead and Zinc Interactions in the Environment, *Int. J. Environ. Pollut.*, 23, 417-424, **2005.**

[33] Ibrahim M., Mahmoud A.A., Computational Notes on the Reactivity of some Functional Groups, J. *Comput. Theor. Nanosci*., 6, 1523-1526, **2009.**

[34] Politzer P., Laurence P.R., Jayasuriya K., Molecular electrostatic potentials: an effective tool for the elucidation of biochemical phenomena, *Environ. Health Persp*., 61, 191-202, **1985.**

[35] Politzer P., Murray J.S., In Murray, J.S. and Sen, K. (Eds) Molecular Electrostatic Potentials. Concepts and Applications, *Elsevier*, Amsterdam, 649-660, **1996.**

[36] Ezzat H., Badry R., Yahia I.S., Zahran H.Y., Elhaes H., Ibrahim M.A., Mapping the molecular electrostatic potential of carbon nanotubes, *Biointerface Research in Applied Chemistry*, 8, 3539-3542, **2018.**

[37] Dedkov Y., Voloshina E., Spectroscopic and DFT studies of graphene intercalation systems on metals, *J. Electron. Spectrosc.*, 219, 77-85, **2017**.

[38] Üngördü A., Tezer N., DFT study on metal-mediated uracil base pair complexes, *J. Saudi Chem. Soc.*, 21(7), 837-844, **2017**.

[39] Khoutoul M., Lamsayah M., Al-blewi F. F., Rezkib N., Aouad M. R., Mouslim M., Touzani R., Liquid–liquid extraction of metal ions, DFT and TD-DFT analysis of some 1,2,4-triazole Schiff Bases with high selectivity for Pb(II) and Fe(II), *J. Mol. Struct.*, 1113, 99-107, **2016**.

[40] Fischer M., DFT-based evaluation of porous metal formates for the storage and separation of small molecules, *Micropor. Mesopor. Mat.*, 219, 249-257, **2016**.

[41] Wang W., Fan L., Wang G., Li Y., CO_2 and SO_2 sorption on the alkali metals doped CaO(100)surface: A DFT-D study, *Appl. Surf. Sci.*, 425, 972-977, **2017**.